Estuarine, Coastal and Shelf Science 198 (2017) 393–399

Contents lists available at ScienceDirect

Estuarine, Coastal and Shelf Science

journal homepage: www.elsevier.com/locate/ecss

Non-local drivers of the summer hypoxia in the East China Sea off the Changjiang Estuary

Wei Qian [a, b], Minhan Dai [a, *], Min Xu [a], Shuh-ji Kao [a], Chuanjun Du [a], Jinwen Liu [a, c], Hongjie Wang [a, d], Liguo Guo [a], Lifang Wang [a]

[a] State Key Laboratory of Marine Environmental Science, Xiamen University, Xiamen 361100, China
[b] College of Geographical Sciences and Institute of Geography, Fujian Normal University, Fuzhou 350007, China
[c] Third Institute of Oceanography, State Oceanic Administration, Xiamen 361005, China
[d] Department of Physical & Environmental Science, Texas A & M University-Corpus Christi, USA

ARTICLE INFO

Article history:
Received 19 November 2015
Received in revised form
19 August 2016
Accepted 27 August 2016
Available online 28 August 2016

Keywords:
Changjiang (Yangtze River) Estuary
Dissolved oxygen
East China Sea
Hypoxia
Shelf-offshore interaction

ABSTRACT

The East China Sea (ECS) off the Changjiang (Yangtze River) Estuary, located around the near field of the Changjiang plume (CJP) is a hot spot where phytoplankton blooms in the surface water and hypoxias in the subsurface/bottom waters are frequently observed. Based on field observations conducted in summer 2009 and 2011, we examined non-local drivers associated with the initial dissolved oxygen (DO) levels that had significant impact on the development of summer hypoxias in the ECS off the Changjiang Estuary. The bottom water mass therein could be traced isopycnally at $24.2 < \sigma_\theta < 25.2$ back to the vicinity of the Luzon Strait, ~1300 km upstream, where subsurface Kuroshio water (~220 m deep with ~190 μmol DO kg^{-1}) mixed with the South China Sea subsurface water (~120 m deep with ~130 μmol DO kg^{-1}). Owing to the difference in DO of these two source water masses, their mixing ratio ultimately determined the initial DO supply to the ECS bottom water that eventually reached the hypoxic zone. This water mass mixture was also subject to biogeochemical alteration during its travel (~60 days) after it intruded into the ECS at the northeastern tip of Taiwan. Along the pathway of the intruded bottom-hugging water, we found systematic increases in nutrient concentrations and apparent oxygen utilization, or drawdown in DO following Redfield stoichiometry as a result of marine organic matter decomposition. These non-local factors exerted a synergistic control on the initial DO of CJP bottom water promoting hypoxia formation, although the residence time of the CJP bottom water was relatively short (~11 days). We contend that such far field drivers should be taken into account in order to better predict the future scenarios of coastal hypoxias in the context of global warming.

© 2016 Elsevier Ltd. All rights reserved.

1. Introduction

Coastal hypoxia, defined as dissolved oxygen (DO) levels <2 mg l^{-1}, is an environmental issue of global concern. Around 400 coastal hypoxic zones collectively occupy ~245,000 km^2 in the coastal oceans of the world (Diaz and Rosenberg, 2008). A number of physical, chemical and biological factors for hypoxia development, such as water column stratification, excessive biomass production stimulated by nutrients and allochthonous organic matter input, have been extensively examined (Bianchi et al., 2010; Boesch et al., 2009; Carstensen et al., 2014; Dai et al., 2006; Green et al., 2006; Rabalais et al., 2014; Rabouille et al., 2008; Wang et al., 2016). Obviously, the formation and maintenance of any hypoxic conditions are also related to the initial DO level which is dependent upon the source of the water masses and biogeochemical reactions along the pathway of the input. However, such impacts of non-local drivers on coastal hypoxia have rarely been mentioned elsewhere, except for a few with solid evidence. For example, upwelling of oxygen depleted subsurface water triggers recurrent hypoxias in coastal regions off New Jersey, Oregon and Namibia, where upwelling of oceanic water provides lower initial DO (Glenn et al., 2004; Grantham et al., 2004; Monteiro et al., 2006), while replete nutrients further drawdown the oxygen level in the coastal system by remineralization of the stimulated biomass when settling down to the subsurface.

Similar to the well-known hypoxic regions such as the Gulf of

* Corresponding author.
E-mail address: mdai@xmu.edu.cn (M. Dai).

http://dx.doi.org/10.1016/j.ecss.2016.08.032
0272-7714/© 2016 Elsevier Ltd. All rights reserved.

Mexico and Chesapeake Bay, summer hypoxia in the East China Sea (ECS) off the Changjiang (Yangtze River) Estuary has been frequently observed and reported in the last decade, and is one of the largest coastal oxygen-depleted areas in the world (Chen et al., 2007). The increasing riverine nutrients loading during past decades exhibit an intimate link with the augmentation in frequency and intensity of oxygen depletion in the coastal bottom water off the estuary (Gong et al., 2011; Wang et al., 2016). Zhu et al. (2011) reported different chemical hydrological characteristics and proposed mechanisms for oxygen depletion in the southern and northern areas off the Changjiang Estuary. Local topography is also regarded as a factor influencing the residence times of the water body to become hypoxic (Wang, 2009). However, less understood was how the initial DO inherited from the source water acts as a non-local driver to regulate deoxygenation and promote hypoxia.

In this study, we presented results of two summer field surveys off the Changjiang Estuary and in the ECS during 2009 and 2011. In examining the coastal hypoxias, the evolution of the bottom water, including DO and nutrients, from its source locations and on its pathway to the hypoxic zone of interest, was examined in order to demonstrate the importance of the origin of the water masses and the biogeochemical alteration along its pathway to the hypoxic zone. Our study highlighted that in addition to the relatively well-studied local factors, the importance of non-local drivers in examining the evolution, occurrence and future status of the seasonal hypoxia in the ECS off the Changjiang Estuary, one of the largest coastal hypoxic zones in the world.

2. Material and methods

2.1. Study area

The ECS is one of the largest marginal seas of the Pacific with a very wide shelf (maximum ~600 km). The water on the ECS shelf is mainly mixed by three prominent water masses (Fig. 1): Changjiang diluted water (CJW) originating from the freshwater runoff from the Changjiang; the Taiwan Warm Current (TWC); and the Kuroshio Current (KC). Changjiang discharges ~9 × 10^{11} m^3 yr^{-1} freshwater together with a large amount of sediments (~2.5 × 10^{14} g yr^{-1}), nutrients (~9 × 10^{11} g yr^{-1} for NO^{3-}; ~2 × 10^{-10} g yr^{-1} for PO_4^{3-}) and organic matter (~3 × 10^{12} g C yr^{-1}) (Yang et al., 2006, Liu et al., 2009; Wang et al., 2012). In the southern ECS, the nearshore Kuroshio branch (NSKB) bifurcates from the main stream of the KC at the shelf-break northeast of Taiwan and intrudes to the ECS shelf towards the Changjiang plume (CJP) region in summer, while the TWC flows northeastward on the top of the NSKB (Yang et al., 2011 and references therein). The intruded water is believed to fuel the high productivity in the ECS (Yang et al., 2013). Meanwhile, the South China Sea (SCS) subsurface water flows out of the Luzon Strait, joining the mainstream of the Kuroshio as another oceanic water source for the ECS shelf (Chen et al., 1995; Chen and Wang, 1999; Chou et al., 2007; Sheu et al., 2009). The Chl a ranged 30–110 mg m^2 and the primary production may reach ~1 g C m^2 day^{-1} in the river plume (Gong et al., 2003). Away from the river plume, primarily productivity is much lower but with high spatial and temporal variability (Chen et al., 2004).

2.2. Cruises and sampling

We conducted two cruises, one onboard the R/V *Dongfanghong II* from Aug.15 to Sept. 2, 2009, and the other the R/V *Runjiang I* from Aug. 15 to 24, 2011. The sampling area covered from the southern ECS to off the Changjiang Estuary, with one along shore transect (T2) and four cross shelf transects (KP, DH5, DH3, T1). The five transects covered from the north of the Taiwan Strait to off the Changjiang Estuary where the three prominent water masses, i.e. TWC, NSKB and CJW, interact. Meanwhile during the 2011 summer cruise, the two northernmost transects off the Changjiang Estuary (T1, T2) were investigated (Hsiao et al., 2014; Tseng et al., 2014) and we repeatedly sampled the second transect (T2). Note that background hydrographic data collected along transects T1 and T2 from the 2011 cruise are partially reported by Tseng et al. (2014) and Hsiao et al. (2014) but from different perspectives.

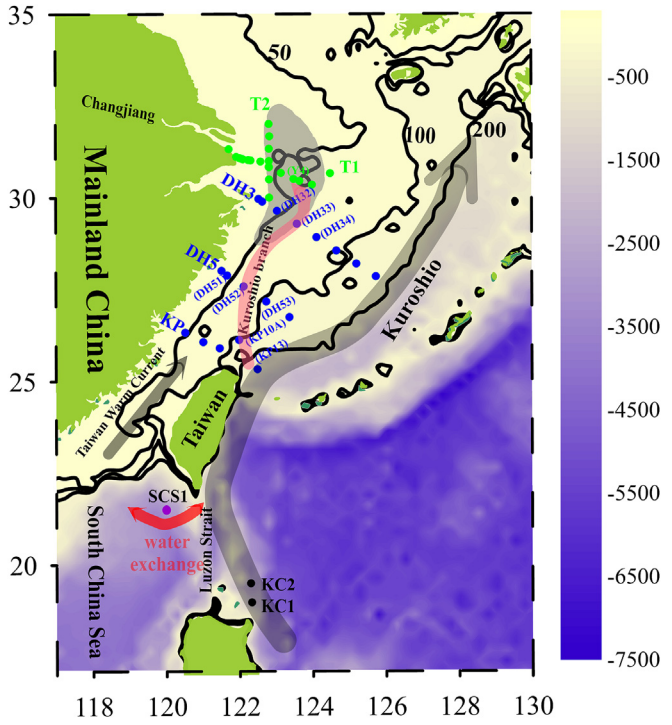

Fig. 1. Map of the East China Sea and adjacent oceanic region showing the topography and locations of the sampling stations during summer cruises in 2009 (blue dots) and 2011 (green dots). The additional stations of SCS1 (purple dot), KC1 and KC2 (grey dots) near the Luzon Strait, representing source oceanic waters collected during a 2010 cruise are redrawn from Du et al. (2013). KP, DH5, DH3, T1 and T2 are also marked as the transect names. Also shown schematically with arrows are the Kuroshio, water exchanges near the Luzon Strait, nearshore Kuroshio branch and Taiwan Warm Current. All stations along the pathway of the nearshore Kuroshio branch are marked with names in parentheses. Depth contours of 50, 100 and 200 m are sketched by grey lines with numbers. The shadowed area off the Changjiang Estuary indicates the hypoxic zone reported by Li et al. (2002). (For interpretation of the references to colour in this figure legend, the reader is referred to the web version of this article.)

Water samples were collected from different depths using Niskin/GoFlo bottles mounted onto a Rosette sampling assembly, equipped with a conductivity-temperature–depth recorder (Sea-Bird 911 plus CTD) for 2009 and 2011 cruise. Analytical protocols for nitrate plus nitrite (N + N) and DIP (dissolved inorganic phosphate) followed Han et al. (2012). The Winkler titration method was applied for DO determination (Zhai et al., 2005). The detection limits for N + N, DIP and DO were 0.1, 0.05 and 0.5 μmol kg^{-1}. Hydrographic data from three stations near the Luzon Strait (KC1, KC2 and SCS1, in Fig. 1), are also presented to demonstrate the influence of the upstream KC and the potential contribution of water from the SCS (Du et al., 2013).

3. Results and discussion

3.1. Chemical hydrography and water mass characterization

Fig. 2 presents the transectional distributions of salinity,

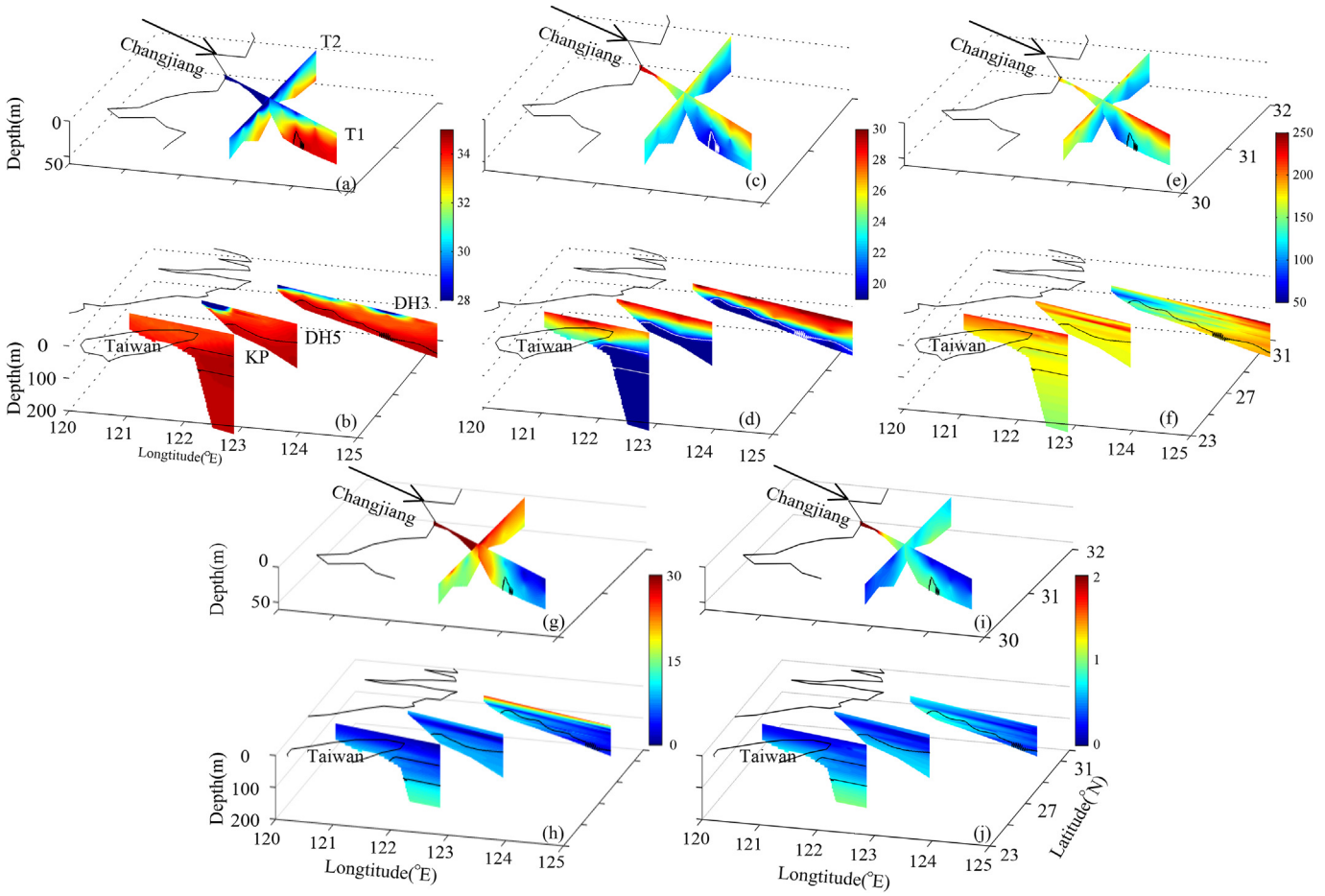

Fig. 2. Transectional distributions of (a), (b) for salinity; (c), (d) potential temperature (°C); (e), (f) DO (μmol kg^{-1}); (g), (h) N + N(μmol kg^{-1}); and (i), (j) DIP (μmol kg^{-1}) selected from 2011 to 2009 summer cruises, respectively. Note that the transectional data of salinity, temperature and nutrients are partially reported by Yang et al. (2011, 2012) and Tseng et al. (2014). The low salinity (<28) and high N + N (>30 μmol kg^{-1}) data were not further differentiated with color and the deep water (>200 m at the easternmost station of the KP transect) were not shown for simplification. The isopycnal surfaces of σ_θ = 24.2, 25.2 (if it existed) are denoted with grey or white curves in each subplot.

potential temperature, DO and nutrients based on the cruises in 2009 and 2011. Low salinity water (S < 30) was confined within the nearshore surface off the Changjiang Estuary, presenting the influence of river discharge. The most saline water (S > 34) was distributed at the subsurface off the northeastern tip of Taiwan and extended to near the bottom at the northern transects (e.g. DH5 and DH3 in Fig. 2b). The warm water mass (θ > 25 °C) occupied most of the surface of the region under survey and the cold water (θ < 19 °C) was observed below ~100 m at the east of the KP transect. Similar to the high salinity water distribution, the cold water also extended northward to transect DH3 near the bottom. The isopycnal surfaces (i.e. σ_θ = 24.2, 25.2, grey or white curves in Fig. 2) revealed a clear spatial distribution for the cool and saline water while a warm and less saline water, the TWC water (Fig. 1) was distributed on top of the cooler and saline water.

As for DO (Fig. 2e–f), most surface values were ~200 μmol kg^{-1} but there were two low DO centers in the subsurface water. One was located off the Changjiang Estuary where seasonal hypoxia is frequently observed (Li et al., 2002; Wei et al., 2007; Zhu et al., 2011). The other center was at ~150 m depth off the northeastern tip of Taiwan where the DO was ~160 μmol kg^{-1}.

The transectional distributions of N + N and DIP throughout the region investigated are displayed in Fig. 2g–j. Nutrient-depleted water (<0.3 μmol kg^{-1} for N + N, <0.2 μmol kg^{-1} for DIP) dominated most of the surface water of the ECS except the area nearshore and off the Changjiang Estuary which is influenced by the riverine input where the N + N was >100 μmol kg^{-1} and the DIP >2 μmol kg^{-1}. Nutrient replete waters (N + N > 7 μmol kg^{-1}, DIP > 0.5 μmol kg^{-1}) were also observed in the subsurface water at the shelf-break northeast of Taiwan and in bottom water on the shelf where the low DO water was located.

Fig. 3 is the θ–S diagram based on the data collected during the two cruises in the ECS and the oceanic stations near Luzon Strait in this study. The ECS continental shelf water mostly had a narrow range in salinity, between 33 and 34, with exceptions in the nearshore mixing zone influenced by the fresh water input and thus with low salinity of <30. Temperature had a much larger range between ~2 and ~30 °C. Nevertheless, most data points fell within a triangular field constrained by three end members, i.e., CJW, ECS shelf water and ECS bottom water (EBW).

In order to trace the source of the EBW, the θ–S of profiles from the typical KC and SCS are also included in Fig. 3a–b. Noteworthy is that the bottom water underneath the plume and of the transects KP, DH5 and DH3 on the ECS shelf, as well as the subsurface water of the SCS1, KC1 and KC2, converged at 24.2 < σ_θ < 25.2 (red quadrilateral in Fig. 3a–b). This suggested that the bottom-hugging water extending from the shelf-break northeast of Taiwan down to the CJP originated from the KC, SCS or their mixture. Fig. 3 also suggested that the TWC contributed little to the bottom water mass of the hypoxic zone. To prove this, we zoomed in on the salinity

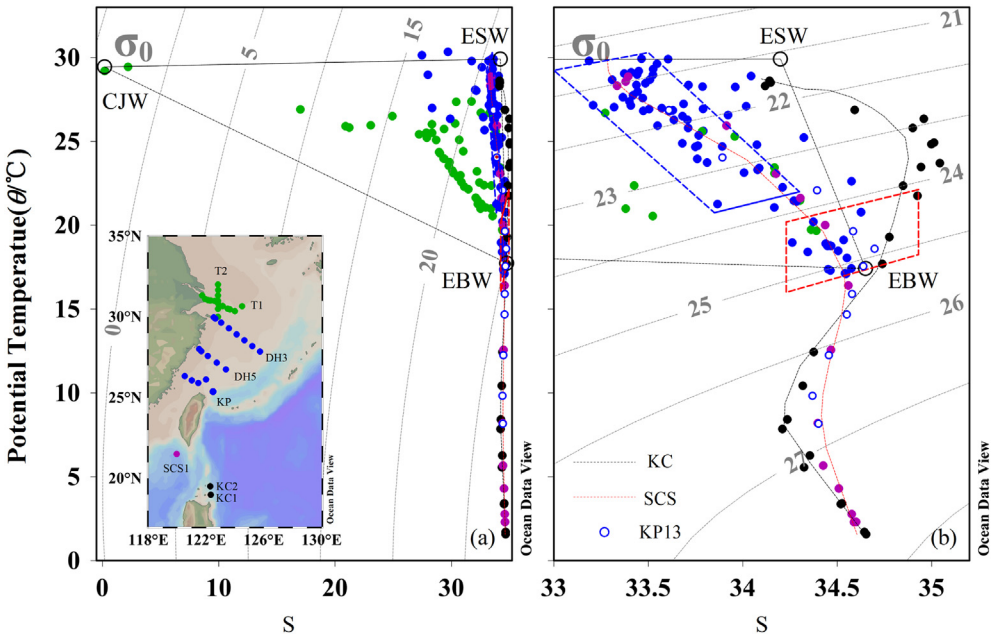

Fig. 3. (a) The potential temperature (θ/°C) vs. salinity scheme for the stations of the 2009 summer cruise (blue) and 2011 summer cruise (green). Also shown are the additional oceanic stations SCS1 (purple), KC1 and KC2 (grey). The three open dots connected by grey dashed lines denote the three end members, i.e. Changjiang water (CJW), ECS surface water (ESW) and ECS bottom water (EBW); and (b) the same data set with the 33–35 salinity scale. The blue quadrilateral contains shelf water with high temperature ($\theta > 20$ °C) and saline ($33 < S < 34$) water; and the red one intruded water featured with the criterion ($24.2 < \sigma_\theta < 25.2$). Also shown are the typical profiles of the Kuroshio (grey dashed line), the SCS (purple dashed line) (Du et al., 2013) and the easternmost station of the KP transect (KP13) is highlighted with open circles. (For interpretation of the references to colour in this figure legend, the reader is referred to the web version of this article.)

scale of 33–35 (Fig. 3b) to examine the fine structure of the water mass composition. The uppermost layer of shelf water within the blue quadrilateral was characterized by higher temperature ($\theta > 20$ °C) and lower salinity ($S < 34$) which was closer to the SCS type implying that it held more SCS and fewer KC properties. Noteworthy, the potential density anomaly (σ_θ) was less than 23.5 for the three stations located just north of the Taiwan Strait, which was consistent with the fact that warm and less saline SCS surface water ($\sigma_\theta < 23.5$ in this work) passes through the Taiwan Strait contributing to the TWC during summer (Jan et al., 2006).

However, the EBW with a characteristic temperature of ~19 °C and salinity of >34, or $\sigma_\theta > 24.2$ would be traceable immediately to the subsurface of the easternmost two stations of the KP and northward transects. Moreover, the θ-S data of the subsurface water during the two surveys ($24.2 < \sigma_\theta < 25.2$) largely fell between those of the typical SCS and the KC especially for those of KP13, the easternmost station of the KP transect. We thus suggested that the bottom water of the hypoxic zone is primarily sourced from the mixture of the KC and SCS subsurface waters which intrude into the ECS via the shelf-break northeast of Taiwan.

Our results were consistent with Yang et al. (2012, 2013), who propose a NSKB, bifurcating from the mainstream of the KC, flowing northwestward beneath the TWC, ultimately reaching 31°N off the mouth of the Changjiang Estuary. We further adopted the explanation of the SCS water emergence on the western boundary of the KC mainstream (Chen, 2005; Chou et al., 2007; Hsin et al., 2012; Shaw, 1991; Sheu et al., 2009; Yang et al., 2011). In comparison with those of the KC, the nutrient enrichment and DO depletion can be clearly determined in the SCS subsurface layer, attributed to basin-wide upwelling internal to the SCS and organic matter remineralization (Dai et al., 2013; Du et al., 2013; Gong et al., 1992).

It was critical, in this work, to evaluate the respective contribution from the possible sources, the Kuroshio and SCS waters, to the EBW. We applied the isopyncal mixing algebra algorithm to the subsurface water of two easternmost stations on transect KP where the intruding water was found to quantify the fractional contribution from each source water (Du et al., 2013). The mixing model is based on mass balance of salinity and θ during the water mass mixing of the two end members, as follows:

$$R_s \times X_s + R_k \times X_k = X_{insitu} \quad (1)$$

$$R_s + R_k = 1 \quad (2)$$

where X_{insitu}, X_s and X_k stand for the salinity (or θ) in the in situ sample, SCS and Kuroshio water that possessed an identical density value. R_s and R_k represent the percentage contribution from the end-members of the SCS and the Kuroshio, which could be solved based on Equations (3) and (4):

$$R_s = \frac{X_k - X_{insitu}}{X_k - X_s} \quad (3)$$

$$R_k = \frac{X_{insitu} - X_s}{X_k - X_s} \quad (4)$$

At the easternmost station (KP13), the two source water masses contributed ~50% to the subsurface water mixture. At station KP10A within the given criterion ($24.2 < \sigma_\theta < 25.2$), a greater SCS fraction of ~90% was revealed.

Since the flow rate for the intruding water is ~1.4 Sv (Yang et al., 2011), we further estimated that the SCS water contributed ~50% of the intruding water based on the above mentioned isopycnal mixing results. It should be pointed out that the SCS subsurface water contained substantially higher levels of nutrients (~10 μmol kg^{-1} for N + N, ~0.66 μmol kg^{-1} for DIP) and apparent oxygen utilization (AOU = $[O_2]_{eq}-[O_2]$, where $[O_2]_{eq}$ is the DO solubility at equilibrium with the atmosphere, $[O_2]$ is in situ DO

concentration) than those of the KC at σ_θ = 24.2–25.2. Therefore the additional nutrient flux of ~7 kmol s^{-1} for N + N and ~0.4 kmol s^{-1} for DIP induced by the SCS water amounted to ~2 folds for the N + N and ~10 folds for the DIP flux from the Changjiang River during summer (Chen and Wang, 1999; Zhou et al., 2008). In addition to the winter nutrient transport from the ECS to the SCS, this process also shed light on another crucial linkage and potential inter-influence between these two major marginal seas in the Western Pacific Ocean via coastal currents (Chou et al., 2007; Han et al., 2013; Sheu et al., 2009).

Taking the hydrological and biogeochemical properties together, we suggested that the EBW originated from the mixture of Kuroshio and SCS subsurface waters, and this source function was a critical determinant of the initial conditions for the hypoxic zone in the ECS off the Changjiang Estuary.

3.2. Evolution of stoichiometry along the pathway on the ECS shelf to the hypoxic zone

We found a significant correlation between N + N and DIP (Fig. 4a) in waters at σ_θ = 24.2–25.2 along the pathway from the Luzon Strait to the region off the Changjiang Estuary. The regression slope of 14.2 ± 0.7 resembled the Redfield ratio implying that the nutrient accumulation in the water was caused mainly by organic matter remineralization.

It was very clear that the AOU values were lower in the KC water compared to those of the typical SCS water within our density criterion (Fig. 4a). The AOU value at station SCS1 was between those of the KC and SCS which suggested mixture of the two source waters. Along the pathway of the NSKB, the AOU generally displayed an increasing pattern from ~60 to ~100 μmol kg^{-1} on the ECS continental shelf.

Transect DH3 extended ~400 km off shore with relatively lower AOU values of ~50 μmol kg^{-1} at σ_θ = ~24.2 at the easternmost stations. At the nearshore stations of the transect, AOU of ~100 μmol kg^{-1} was determined at σ_θ = ~24.6. This considerable AOU fluctuation was observed within the density criterion of interest throughout transect DH3 due to the difference in initial AOU in the source waters and the varying oxygen consumption along the NSKB pathway. For example, the west boundary of the KC water, holding more fractions of the SCS water, was more likely to intrude into the ECS. In addition, when the NSKB flowed northward, it received more organic matter along the productive inner shelf of the ECS before it reached the vicinity of the Changjiang Estuary (Chen et al., 2004; Yang et al., 2011), resulting in significant increases in AOU given the long travel time for the NSKB from the intruding point at the shelf-break northeast of Taiwan to the vicinity off the Changjiang River (~60 days, Yang et al., 2013).

Given that the total AOU increment was ~40 μmol kg^{-1} on the continental shelf of the ECS, the DO drawdown rate could be estimated to be ~0.67 μmol kg^{-1} day^{-1} (40 μmol kg^{-1}/60 days), which is equivalent to a supplying rate of organic carbon of ~0.12 g C m^{-2} day^{-1} assuming the bottom water was ~20 m thick and if the classical molar respiration quotient (O_2/C = 1.3) was taken. This DO drawdown on the ECS shelf seemed to be sufficiently supported by the organic matter induced from reported new productivity of 0.06–2.22 g C m^{-2} d^{-1} (Chen et al., 2004). This suggested that the observed drawdown in DO along the pathway of the NSKB was reasonable.

On the other hand, the bottom water respiration and sediment oxygen demand were regarded as a crucial DO sink. While the total DO consumption rate ranged from ~2 to ~8 μmol O_2 kg^{-1} d^{-1} underneath the CJP (Cai et al., 2014; Liu, 2014), if a 20 m thick bottom water and residence time was ~11 days (Li et al., 2002; Rabouille et al., 2008), less than ~90 μmol O_2 kg^{-1} (2–8 μmol O_2 kg^{-1} d^{-1} × 11 day = 22–88 μmol O_2 kg^{-1}) consumption was

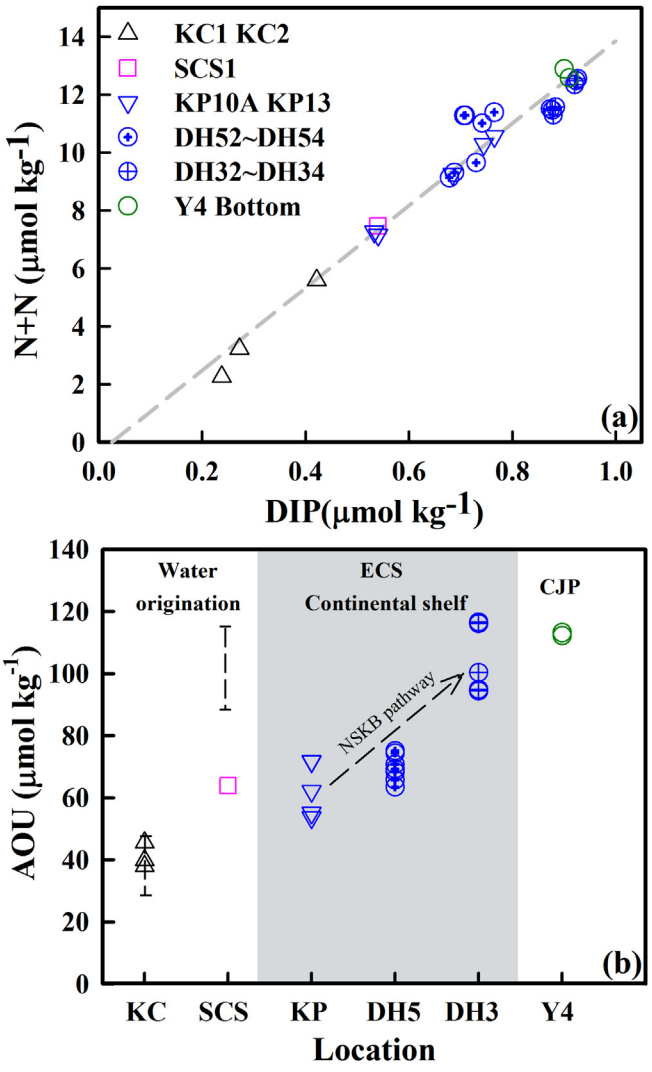

Fig. 4. (a) Correlation between DIP and N + N with the potential density anomaly between 24.2 and 25.2 within the ECS continental shelf based on the data collected during the 2009 and 2011 surveys. Additional oceanic stations near the Luzon Strait (SCS1, KC1 and KC2) are also displayed. The grey dashed line denotes the regression curve between DIP and N + N, N + N=(14.2 ± 0.7)DIP + (-0.4 ± 0.5), r^2 = 0.95, n = 25, p < 0.0001; and (b) the AOU evolution along the pathway. The shadowed rectangle divides the investigated area into three domains, i.e. water mass source regime, continental shelf of the ECS, and off the Changjiang Estuary. The AOU range for the subsurface water at 24.2 < σ_θ < 25.2 of the typical KC and SCS (Du et al., 2013) is also shown. The pathway of the nearshore Kuroshio branch is schematically indicated by an arrow. The offshore stations of DH3 were excluded because of their deviation from the pathway.

expected under the river plume. This first order estimation further suggested that the initial DO of the source water masses and the DO consumption along the pathway to the hypoxic zone indeed played a significant role in the formation and development of the hypoxias.

In order to well summarize the whole pathway of the bottom water, all key processes were emphasized in Fig. 1. The upstream KC mixes with water flowing out from the SCS and then flows northward into the ECS as an intrusion, where the nearshore branch bifurcates from the KC mainstream and keeps flowing northwestward until it reaches the region off the Changjiang Estuary around 31°N.

4. Concluding remarks

This study examined the far field controls on the initial DO levels

of the water masses supplied to the hypoxic zone. We have demonstrated that the source function of the initial water masses that fueled the bottom ECS water mass was an important determinant. Equally important was the oxygen consumption along the pathway on the shelf of the ECS, which was largely determined by the surface biogeochemical processes related to biomass production and its sinking and decomposition.

We postulated that this initial DO condition would be expected to play an even more important role in the global warming scenario in controlling the summer hypoxia off the Changjiang Estuary. For instance, a substantial increase of sea surface temperature, particularly in the western Pacific, would result in an intensified stratification and a decrease in oxygen solubility, which would further exacerbate the oxygenation status of the intermediate water (Carstensen et al., 2014; Helm et al., 2011; Jaccard and Galbraith, 2011; Keeling and Garcia, 2002; Stramma et al., 2009). Indeed, Lui et al. (2014), based on long-term data analysis, report a decreasing DO trend in the Kuroshio intermediate water with increasing nutrients due to reduced ventilation. The even lower initial DO in the source water would certainly impact the baseline DO in the coastal hypoxic zones, including the region off the Changjiang Estuary, where bottom water is brought by oceanic subsurface upwelling water.

Acknowledgements

This research was supported by the National Basic Research Program of China (973 Program) through grant 2015CB954001 and the Ocean Public Welfare Scientific Research Project, State Oceanic Administration, People's Republic of China through grant 2015418003-3. This study was also partially supported by the National Natural Science Foundation of China (NSFC) through grant 91328202 and 41130857. We thank Qian Li, Chao Zhang, Pinghe Cai, Hua Lin and Huade Zhao for their comments. John Hodgkiss is thanked for his assistance with English. We are also grateful to the captains, crews, and technicians of *R/V Runjiang I* and *Dongfanghong II* for their support and laboratory assistance.

References

Bianchi, T.S., DiMarco, S.F., Cowan Jr., J.H., Hetland, R.D., Chapman, P., Day, J.W., Allison, M.A., 2010. The science of hypoxia in the northern Gulf of Mexico: a review. Sci. Total Environ. 408, 1471–1484.

Boesch, D.F., Boynton, W.R., Crowder, L.B., Diaz, R.J., Howarth, R.W., Mee, L.D., Nixon, S.W., Rabalais, N.N., Rosenberg, R.J., Sanders, G., Scavia, D., Turner, R.E., 2009. Nutrient enrichment drives Gulf of Mexico hypoxia. EOS Trans. Am. Geophys. Union 90, 117–118.

Cai, P.H., Shi, X.M., Moore, W.S., Peng, S.Y., Wang, G.Z., Dai, M.H., 2014. ^{224}Ra:^{228}Th disequilibrium in coastal sediments: implications for solute transfer across the sediment-water interface. Geochim. Cosmochim. Acta 125, 68–84.

Carstensen, J., Andersen, J.H., Gustafsson, B.G., Conley, D.J., 2014. Deoxygenation of the Baltic sea during the last century. Proc. Natl. Acad. Sci. U. S. A. 111, 5628–5633.

Chen, C.-C., Gong, G.-C., Shiah, F.-K., 2007. Hypoxia in the East China Sea: one of the largest coastal low-oxygen areas in the world. Mar. Environ. Res. 64, 399–408.

Chen, C.-T.A., 2005. Tracing tropical and intermediate waters from the South China Sea to the Okinawa trough and beyond. J. Geophys. Res. 110, C05012.

Chen, C.-T.A., Wang, S.-L., 1999. Carbon, alkalinity and nutrient budgets on the East China Sea continental shelf. J. Geophys. Res. 104, 20675–20686.

Chen, C.-T.A., Ruo, R., Pai, S.C., Liu, C.T., Wong, G.T.F., 1995. Exchange of water masses between the East China Sea and the Kuroshio off northeastern Taiwan. Cont. Shelf Res. 15, 19–39.

Chen, Y.-L.L., Chen, H.-Y., Gong, G.-C., Lin, Y.-H., Jan, S., Takahashi, M., 2004. Phytoplankton production during a summer coastal upwelling in the East China Sea. Cont. Shelf Res. 24, 1321–1338.

Chou, W.-C., Sheu, D.D., Chen, C.-T.A., Wen, L.-S., Yang, Y., Wei, C.-L., 2007. Transport of the South China Sea subsurface water outflow and its influence on carbon chemistry of Kuroshio waters off southeastern Taiwan. J. Geophys. Res. 112, C12008.

Dai, M.H., Cao, Z.M., Guo, X.H., Zhai, W.D., Liu, Z.Y., Yin, Z.Q., Xu, Y.P., Gan, J.P., Hu, J.Y., Du, C.J., 2013. Why are some marginal seas sources of atmospheric CO_2? Geophys. Res. Lett. 40, 2154–2158.

Dai, M.H., Guo, X.H., Zhai, W.D., Yuan, L.Y., Wang, B.W., Wang, L.F., Cai, P.H., Tang, T.T., Cai, W.-J., 2006. Oxygen depletion in the upper reach of the Pearl River estuary during a winter drought. Mar. Chem. 102, 159–169.

Diaz, R.J., Rosenberg, R., 2008. Spreading dead zones and consequences for marine ecosystems. Science 321, 926–929.

Du, C., Liu, Z., Dai, M., Kao, S.-J., Cao, Z., Zhang, Y., Huang, T., Wang, L., Li, Y., 2013. Impact of the Kuroshio intrusion on the nutrient inventory in the upper northern South China Sea: insights from an isopycnal mixing model. Biogeosciences 10, 6419–6432.

Glenn, S., Arnone, R., Bergmann, T., Bissett, W.P., Crowley, M., Cullen, J., Gryzmski, J., Haidvogel, D., Kohut, J., Moline, M., Oliver, M., Orrico, C., Sherrell, R., Song, T., Weidemann, A., Chant, R., Schofield, O., 2004. Biogeochemical impact of summertime coastal upwelling on the New Jersey shelf. J. Geophys. Res. 109, C12S02.

Gong, G.-C., Liu, K.-K., Liu, C.-T., Pai, S.-C., 1992. The chemical hydrography of the South China Sea West of Luzon and a comparison with the West Philippine Sea. Terr. Atmos. Ocean. Sci. 3, 587–602.

Gong, G.-C., Wen, Y.-H., Wang, B.-W., Liu, G.-J., 2003. Seasonal variation of chlorophyll a concentration, primary production and environmental conditions in the subtropical East China Sea. Deep Sea Res. 50, 1219–1236.

Gong, G.-C., Liu, K.-K., Chiang, K.-P., Hsiung, T.-M., Chang, J., Chen, C.-C., Hung, C.-C., Chou, W.-C., Chung, C.-C., Chen, H.-Y., Shiah, F.-K., Tsai, A.-Y., Hsieh, C.-H., Shiao, J.-C., Tseng, C.-M., Hsu, S.-C., Lee, H.-J., Lee, M.-A., Lin, I.I., Tsai, F., 2011. Yangtze River floods enhance coastal ocean phytoplankton biomass and potential fish production. Geophys. Res. Lett. 38, L13603.

Grantham, B.A., Chan, F., Nielsen, K.J., Fox, D.S., Barth, J.A., Huyer, A., Lubchenco, J., Menge, B.A., 2004. Upwelling-driven nearshore hypoxia signals ecosystem and oceanographic changes in the northeast Pacific. Nature 429, 749–754.

Green, R.E., Bianchi, T.S., Dagg, M.J., Walker, N.D., Breed, G.A., 2006. An organic carbon budget for the Mississippi River turbidity plume and plume contributions to air-sea CO_2 fluxes and bottom water hypoxia. Estuaries Coasts 29, 579–597.

Han, A.Q., Dai, M.H., Kao, S.-J., Gan, J.P., Li, Q., Wang, L., Zhai, W.D., Wang, L., 2012. Nutrient dynamics and biological consumption in a large continental shelf system under the influence of both a river plume and coastal upwelling. Limnol. Oceanogr. 57, 486–502.

Han, A.Q., Dai, M.H., Gan, J.P., Kao, S.-J., Zhao, X.Z., Jan, S., Li, Q., Lin, H., Chen, C.-T.A., Wang, L., Hu, J.Y., Wang, L.F., Gong, F., 2013. Inter-shelf nutrient transport from the East China Sea as a major nutrient source supporting winter primary production on the northeast South China Sea shelf. Biogeosciences 10, 8159–8170.

Helm, K.P., Bindoff, N.L., Church, J.A., 2011. Observed decreases in oxygen content of the global ocean. Geophys. Res. Lett. 38, L23602.

Hsiao, S.S.-Y., Hsu, T.-C., Liu, J.-W., Xie, X., Zhang, Y., Lin, J., Wang, H., Yang, J.-Y.T., Hsu, S.C., Dai, M.H., Kao, S.-J., 2014. Nitrification and its oxygen consumption along the turbid Changjiang River plume. Biogeosciences 11, 2083–2098.

Hsin, Y.-C., Wu, C.-R., Chao, S.-Y., 2012. An updated examination of the Luzon strait transport. J. Geophys. Res. 117, C03022.

Jaccard, S.L., Galbraith, E.D., 2011. Large climate-driven changes of oceanic oxygen concentrations during the last deglaciation. Nat. Geosci. 5, 151–156.

Jan, S., Sheu, D.D., Kuo, H.-M., 2006. Water mass and throughflow transport variability in the Taiwan strait. J. Geophys. Res. 111, C12.

Keeling, R.F., Garcia, H.E., 2002. The change in oceanic O_2 inventory associated with recent global warming. Proc. Natl. Acad. Sci. U. S. A. 99, 7848–7853.

Li, D.J., Zhang, J., Huang, D.J., Wu, Y., Liang, J., 2002. Oxygen depletion off the Changjiang (Yangtze River) Estuary. Sci. China Ser. D Earth Sci. 45, 1137–1146.

Liu, S.M., Hong, G.H., Zhang, J., Ye, X.W., Jiang, X.L., 2009. Nutrient budgets for large Chinese estuaries. Biogeosciences 6, 2245–2263.

Liu, J.W., 2014. On the Respiration and Ocean Acidification in the Coastal Ocean. Xiamen University, Xiamen, China. Ph.D. Thesis.

Lui, H.-K., Chen, C.-T.A., Lee, J., Bai, Y., He, X.Q., 2014. Looming hypoxia on outer shelves caused by reduced ventilation in the open oceans: case study of the East China Sea. Estuar. Coast. Shelf Sci. 151, 355–360.

Monteiro, P.M.S., Van der Plas, A., Mohrholz, V., Mabille, E., Pascall, A., Joubert, W., 2006. Variability of natural hypoxia and methane in a coastal upwelling system: oceanic physics or shelf biology? Geophys. Res. Lett. 33, L16614.

Rabalais, N.N., Cai, W.-J., Carstensen, J., Conley, D.J., Fry, B., Hu, X.P., Quinones-Rivera, Z., Rosenberg, R., Slomp, C.P., Turner, R.E., Voss, M., Wissel, B., Zhang, J., 2014. Eutrophication-driven deoxygenation in the coastal ocean. Oceanography 27, 172–183.

Rabouille, C., Conley, D.J., Dai, M.H., Cai, W.-J., Chen, C.-T.A., Lansard, B., Green, R., Yin, K., Harrison, P.J., Dagg, M., McKee, B., 2008. Comparison of hypoxia among four river-dominated ocean margins: the Changjiang (Yangtze), Mississippi, Pearl, and Rhône Rivers. Cont. Shelf Res. 28, 1527–1537.

Shaw, P.-T., 1991. The seasonal variation of the intrusion of the Philippine Sea water into the South China Sea. J. Geophys. Res. 96, 821–827.

Sheu, D.D., Chou, W.-C., Chen, C.-T.A., Wei, C.-L., Hsieh, H.-L., Hou, W.-P., Dai, M.H., 2009. Riding over the Kuroshio from the south to the East China Sea: mixing and transport of DIC. Geophys. Res. Lett. 36, L07603.

Stramma, L., Visbeck, M., Brandt, P., Tanhua, T., Wallace, D., 2009. Deoxygenation in the oxygen minimum zone of the eastern tropical north Atlantic. Geophys. Res. Lett. 36, L20607.

Tseng, Y.-F., Lin, J., Dai, M., Kao, S.-J., 2014. Joint effect of freshwater plume and coastal upwelling on phytoplankton growth off the Changjiang River. Biogeosciences 11, 409–423.

Wang, B.D., 2009. Hydromorphological mechanisms leading to hypoxia off the

Changjiang Estuary. Mar. Environ. Res. 67, 53–58.
Wang, H.J., Dai, M.H., Liu, J.W., Kao, S.-J., Zhang, C., Cai, W.-J., Wang, G.Z., Qian, W., Zhao, M.X., Sun, Z.Y., 2016. Eutrophication-driven hypoxia in the East China Sea off the Changjiang Estuary. Environ. Sci. Technol. 50, 2255–2263.
Wang, X.C., Ma, H.Q., Li, R.H., Song, Z.S., Wu, J.P., 2012. Seasonal fluxes and source variation of organic carbon transported by two major Chinese Rivers: the Yellow River and Changjiang (Yangtze) River. Glob. Biogeochem. Cycles 26, GB2025.
Wei, H., He, Y.C., Li, Q.J., Liu, Z.Y., Wang, H.T., 2007. Summer hypoxia adjacent to the Changjiang Estuary. J. Mar. Syst. 67, 292–303.
Yang, D.Z., Yin, B.S., Liu, Z.L., Feng, X.R., 2011. Numerical study of the ocean circulation on the East China Sea shelf and a Kuroshio bottom branch northeast of Taiwan in summer. J. Geophys. Res. 116, C05015.
Yang, D.Z., Yin, B.S., Liu, Z.L., Bai, T., Qi, J.F., Chen, H.Y., 2012. Numerical study on the pattern and origins of Kuroshio branches in the bottom water of southern East China Sea in summer. J. Geophys. Res. 117, C02014.
Yang, D.Z., Yin, B.S., Sun, J.C., Zhang, Y., 2013. Numerical study on the origins and the forcing mechanism of the phosphate in upwelling areas off the coast of Zhejiang province. China in summer. J. Mar. Syst. 123, 1–18.
Yang, Z., Wang, H., Saito, Y., Milliman, J.D., Xu, K., Qiao, S., Shi, G., 2006. Dam impacts on the Changjiang (Yangtze) River sediment discharge to the sea: the past 55 years and after the three Gorges dam. Water Resour. Res. 42, W04407.
Zhai, W.D., Dai, M.H., Cai, W.-J., Wang, Y.C., Wang, Z.H., 2005. High partial pressure of CO_2 and its maintaining mechanism in a subtropical Estuary: the Pearl River Estuary, China. Mar. Chem. 93, 21–32.
Zhou, M.J., Shen, Z.L., Yu, R.C., 2008. Responses of a coastal phytoplankton community to increased nutrient input from the Changjiang (Yangtze) River. Cont. Shelf Res. 28, 1483–1489.
Zhu, Z.Y., Zhang, J., Wu, Y.Y., Zhang, Y., Lin, J., Liu, S.M., 2011. Hypoxia off the Changjiang (Yangtze River) Estuary: oxygen depletion and organic matter decomposition. Mar. Chem. 125, 108–116.